48th AIAA Aerospace Sciences Meeting Including the New Horizons Forum and Aerospace Exposition
4 - 7 January 2010, Orlando, Florida
AIAA 2010-1392

Conceptual Design of an Environmentally Responsible 150-Passenger Commercial Aircraft

Natalie R. Smith*, Bryan Blessing*, James Dixon*, Allen Mackey*, Gregory McKenzie*, Robert McDonald†, and Bruce Wright‡
California Polytechnic State University, San Luis Obispo, CA 93407

Verde **is an environmentally responsible commercial transport seating 150 dual-class passengers, designed in response to the 2008-2009 Request for Proposal from the American Institute of Aeronautics and Astronautics Undergraduate Team Aircraft Design Competition. While the airline industry faces increasing pressures from the cost of fuel and the responsibility of environmental impact, the next generation of this aircraft class must operate more efficiently and address those environmental needs. Therefore, all design decisions for *Verde* focused first on reducing fuel burn, second on reducing emissions, then noise, and finally on maintaining flyaway cost, airport integration, and passenger comfort. The final design utilizes several green technologies such as an unducted fan engine cycle, biofuel, and use of advanced yet reusable materials to achieve these goals. Much of the design process focused on trying to increase the main wing aspect ratio which required the need to balance structural weight, aerodynamic performance benefits, and airport integration. This fuel-burn-centered philosophy yielded significant improvements, including a fuel block burn for the typical 500 nmi mission of 38.1 lb/seat and an 10% improvement in operating cost compared to current operations.**

Nomenclature

AR	=	aspect ratio
b	=	span
$BSFC$	=	brake specific fuel consumption
BWB	=	blended wing body
C_D	=	coefficient of drag
C_L	=	coefficient of lift
CG	=	center of gravity
K_a	=	technology factor
L/D	=	lift-to-drag ratio
M_{DD}	=	drag divergence Mach number
M_{crit}	=	critical Mach number
S	=	surface area
t/c	=	thickness-to-chord ratio
$TOGW$	=	takeoff gross weight
$TSFC$	=	thrust specific fuel consumption
Λ	=	sweep angle

1. Introduction

Kermit Design of California Polytechnic State University, San Luis Obispo is proud to present *Verde*, an environmentally responsible commercial transport that seats 150 dual-class passengers, in response to the 2008-2009 Request for Proposal (RFP)[1] from the American Institute of Aeronautics and Astronautics (AIAA) Undergraduate Team Aircraft Design Competition. Kermit Design's objective for this aircraft is to design an efficient airliner, in service by 2018, which will be versatile and reliable while using "green" technology to reduce fuel burn and emissions.

* Aerospace Engineering, One Grand Avenue, AIAA Student Member
† Lockheed Martin Professor, Aerospace Engineering, One Grand Avenue, AIAA Member
‡ Instructor, Aerospace Engineering, Program Manager, SkunkWorks, Retired, AIAA Member

Copyright © 2010 by Natalie Smith. Published by the American Institute of Aeronautics and Astronautics, Inc., with permission.

While the airline industry faces increasing pressures from the cost of fuel and environmental impact, the next generation of this aircraft class must operate more efficiently and address those environmental needs. These demands and requirements illustrated by the RFP are echoed by NASA's Environmentally Responsible Aviation Project[2] which is focusing resources toward the research of "enabling technologies that would have little, if any, negative effect on the environment and global climate". The designers feel that concerns regarding the environment and natural resources will drive the aerospace industry to address improved fuel burn at the cost of some reductions in other areas such as noise. Therefore, all design decisions for *Verde* focused first on reducing fuel burn, second on reducing emissions, then noise, and finally on maintaining flyaway cost, airport integration, and passenger comfort.

2. Initial Design Overview

Initial steps in the design included a mission analysis and constraint diagram. The mission analysis was completed using a regression based historical weight model and fuel fractions for each mission segment, this code was later validated alongside a drag polar validation. The most constraining requirements of the design space were the 140 knot approach velocity, balanced field length of 7,000 ft, and top of climb cruise at 300 ft/min, resulting in a thrust-to-weight of 0.33 and a wing loading of 130 lb/ft^2, shown in Figure 1.

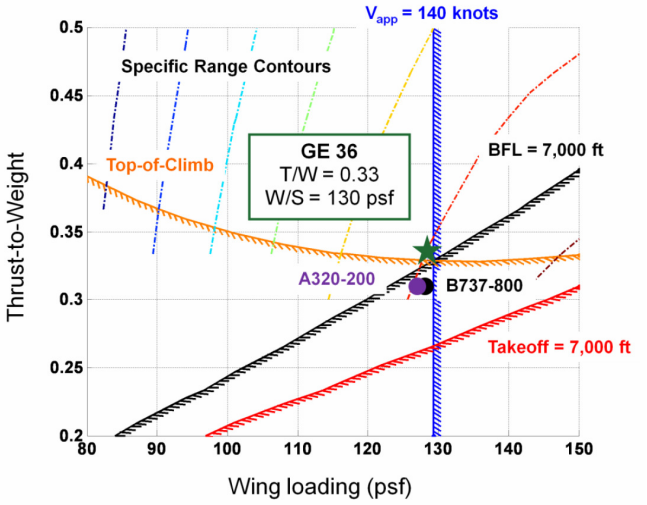

Figure 1: Constraint Diagram showing contours of specific range and the design point

At the onset of this design, the Breguet range equation provided a natural breakdown of the major factors to improve the aircraft efficiency. The three major components, thrust specific fuel consumption (TSFC), lift-to-drag ratio (L/D), and weight fraction were used accordingly to maximize the improvements of the aircraft based on how much each component affected the overall savings.

Basic fuselage type and size was the first characteristic of *Verde* to be defined. A broad fuselage study involved a blended wing body (BWB) and many cylindrical fuselage configurations. Traditionally, the blended wing body configuration has been undesirable for this class of aircraft based to the geometry demands.[3] Kermit Design investigated the BWB geometry needed for this design and found that with a standard BWB seating format the minimal cabin height and most reasonable chord length (30ft) results in a 17% thick root chord. Therefore, Kermit Design focused on a cylindrical fuselage layout. The team considered an array of narrow and wide body configurations and a weight and drag estimate was calculated for each. Initially, the wide body configurations seemed to be the favorable choice, but with a closer look it was found that the drag buildups did no account for base drag. Therefore, 3D CFD was completed on the best seating for each class, narrow and wide, for a better drag comparison, shown in . From this, a narrow body, 3-3 seating configuration was chosen.

Table I: Drag and weight results of fuselage study.

Seating	3 3	3 4 3
Component Buildup $C_{D\,(-)}$	0.0071	0.0078
CFD C_D (-)	0.0074	0.0087
Fuselage Weight (lb)	17,921	14,243

3. Design Iteration Overview

From the analysis summarized in the remainder of this paper, three major iterations resulted. *Iteration 1* was a high strut-braced wing with aft-mounted unducted fans shielded by an H-tail. Originally used as a validation for the benefits of the strut, *Iteration 2* utilized the same empennage with a low wing. Iteration 2 became the primary design because the small improvement in fuel burn with the strut did not buy this unconventional technology onto the aircraft. Finally, Iteration 3, *Verde*, reconfigured the empennage placing the engines at the side of the fuselage with a

T-tail. This decision addressed many concerns about the H-tail, including possible engine fratricide issues, integration, and the aerodynamic, structural, and controllability issues generated by having the two engines so close to one another. All three iterations are pictured in Figure 2.

Figure 2: Design Concepts for *Iteration 1*, *Iteration 2*, and *Verde* (from left to right)

4. Propulsion

As the philosophy and the Bruguet range equation outlined fuel burn or TSFC was the most important area of saving, therefore engine selection was a vital element of the design. Three major engine concepts were considered, including the open rotor concepts from General Electric and CFM International, the geared turbofan from Pratt and Whitney, and the advanced direct-drive turbofan from CFM International. While all three concepts promise improvements over the current engines, the open rotor or unducted fan engine cycle was chosen due to its significant advantages for reduced fuel burn, despite the uncertainty regarding its noise levels.

The propfan takes advantage of the efficiency of a propeller while maintaining the ability to cruise at similar speeds as a turbofan. The counter-rotating propellers allow the second blade row to counteract the swirl effects from the first row, thus straightening the thrust and increasing the efficiency compared to a single rotating propeller.[4] This coupling of ultra high bypass ratio and aerodynamically advanced fan blade design allow the propfan to achieve an advantage in fuel consumption. By nature of this combination, the propfan does have more thrust lapse than the standard high bypass ratio turbofan. Figure 3 shows a carport plot of these parameters.

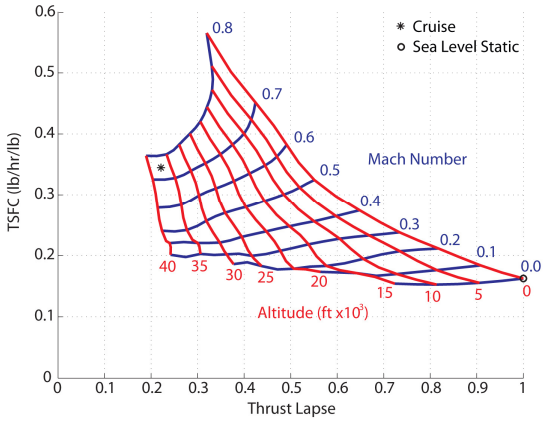

Figure 3: Carpet Plot of Engine Parameters: Thrust Specific Fuel Consumption and Thrust Lapse for the GE 36.

Engine performance was initially analyzed using a rubberized engine deck based on the GE 36, which was generated from General Electric test data provided by Professor Mark Waters. The GE 36 was designed and tested in the 1980s, at which time a F404 turbojet was used as the core.[5] This core is from a particularly aged engine and would not reflect a modern design.

To develop a more sophisticated engine deck, fan sizing from propeller maps and a turboshaft cycle analysis program written by Professor Mark Waters were used to model a counter-rotating unducted fan cycle. The engine was sized at top of climb and restricted to a tip speed of 800 ft/sec. Propeller maps were created using trends from three reports[6,7,8], of which two were for single props while the third addressed counter-rotating trends. Once the required power was known, a turbostaft engine cycle analysis was completed. This program accounted for losses at each component of the engine, including bleed air for the environmental control system (ECS) and reports back brake specific fuel consumption (BSFC) and fuel flow rate. The cycle was then calibrated using the GE 36 data provided by Mark Waters. To reflect a more advanced core some moderate cycle analysis improvements were applied, such as turbine inlet temperature and pressure ratios.[9] No improvements were made to account for any improvements with fan blade efficiencies. Blade design will be greatly affected by the acoustic requirements of this engine; therefore, some engine efficiency may be sacrificed for more optimum noise levels.

Although the engine choice is most desirable for the fuel burn ability, the integration of the engine with the fuselage has been considered such that an airline may chose to install a propfan or a turbofan. This adds to the versatility of the aircraft without much effect on the design. In either case, pylons are mounted aft of the pressure bulk head and are placed vertically to as ensure tail strike occurs prior to engine blade strike.

5. Structures and Materials

Materials selection was primary focused on reducing the structural weight of the aircraft. The use of composites and titanium are increasingly more common on new aircraft. The net structural weight savings accomplished for Verde was 10%. Furthermore, these materials will have the ability to be recycled at the aircraft end of life. Improved passenger comfort is also achieved with the usage of composites in the fuselage, by increased window size and decreased cabin pressure altitude. With the usage of composites, the fuselage thickness is now limited to minimum gage and not by stresses, therefore these improvements are included without any penalty to the design.

The fuselage stringer and ribs spacing was determined using Roskam[10] design texts in the semi-monocoque fashion. This resulted in a rib spacing of 19 inches and stringer spacing of 22 inches. The front spar of the wings is located at 23% of the chord, with the rear spar at 65% of the chord.

6. Weights

The empty weight buildup began with a comparison of two methods to determine wing weight, a historical wing-weight buildup regression from NASA[11] and a quasi-analytical method from SAWE[12], used for the aspect ratio study, which will be discussed in the next section. Validation was completed with a 737-200 and a MD-80 weights, the NASA method provided more accurate weight estimates and with a 5.5% calibration. A 10% structural weight savings was applied to account for use of advanced materials. Torenbeek's[13] method from Roskam[10] was used to determine the weight of the empennage and fuselage. The rest of the fixed weight components were taken to be the same as the 737. From the sum of these components, the total structural weight for *Verde* is approximately 43,000 lb as seen in Table II. Combining the fixed equipment weight with the structural weight yielded an empty weight value of 79,300 lb, and a TOGW of 139,500 lb.

Table II: Structural weight breakdown

(lb)	*Verde*
Wing	15,900
Horizontal Tail	1,650
Vertical Tail	1,390
Fuselage	16,400
Nacelle Group	2,170
Main LG	4,930
Nose LG	560
Total Structural	43,000

To determine the longitudinal and vertical center of gravity (CG) locations of *Verde,* each major component on the aircraft was referenced from a fuselage station (FS) located 5ft ahead of the fuselage nose, and a water line (WL) located 6 ft below the underside of the fuselage. The CG was found to be at an FS of 72.6 ft and a WL of 14.9 ft.

7. Aerodynamics

A. Validation

Validation of the mission analysis and drag polars for *Verde* was completed with DC-10 40 data[14]. Although this aircraft does not represent the same class size of aircraft, extensive data including many drag polars at different Mach numbers and a detailed payload range diagram were available. Two methods were used to validate the drag polar: a drag buildup method from Roskam[15] was used as well as NASA aerodynamics code called Empirical Drag Estimation Tool (EDET) that comes from their packaged Flight Optimization System (FLOPS)[16]. shows all three drag polars. The component buildup method from Roskam did a good job at predicting the drag on the aircraft. While the NASA aerodynamic code EDET overpredicted the addition of viscous drag due to lift and induced drag causing the increase in drag at higher coefficients of lift (C_L). For this reason, the component method was used to predict drag for the project. For the mission validation, a 5,000 nmi mission was selected, because this point was clearly marked on the payload range diagram. The mission analysis overpredicted fuel burn by 3.5%. A correction factor was applied to the mission analysis resulting in predictions of fuel burn within ±1%.

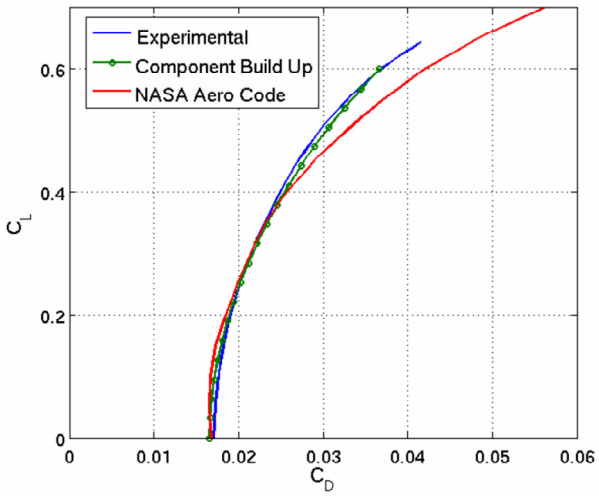

Figure 4: Drag polar validation for the DC-10 40 under cruise conditions of Mach number 0.78 at 38,000 ft

B. Aspect Ratio Study

In order to justify the wing aspect ratio (AR) chosen for *Verde*, an AR trade study was performed and compared versus fuel burn. The methodology used to complete the study was a ten-step process, which starts by picking a design point from the constraint diagram. Then a historical empty weight regression is used to find an initial guess for the empty weight and TOGW of this aircraft. The user determines a range of ARs to analyze from which a wing planform, including optimized sweep, taper, and twist, is determined. The tail is then sized accordingly to match the wing planform. The empty weight buildup calculates the weight of the wing, tail, and fuselage. The design mission is analyzed to find a new TOGW corresponding to the empty weight of the aircraft. This TOGW is fed back into the wing planform to converge on an empty weight for the given AR. Once converged on an empty weight the fuel burn is calculated for the optimization mission. Since 50% of the projected missions are 500 nmi, Kermit Design chose that mission to evaluate the fuel burn. The comparison between a standard low wing and a high strut-braced wing is shown in Figure 5.

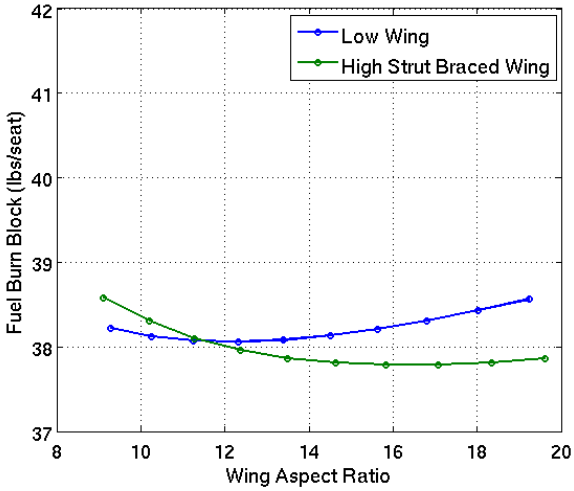

Figure 5: Fuel Burn as a Function of Wing Aspect Ratio for Both a Low Wing and High Strut-Braced Wing for a 500 nmi Mission

C. Wing Planform

The wing planform design focused on selecting an aspect ratio which would accomplish three main goals: maximize the L/D_{cruise}, minimize structural penalties, and maintain a wingspan within the Class III requirement. Next the Korn[17] equation was used to determine the quarter chord sweep, which Equation 2 shows.

$$M_{DD} = \frac{K_a}{\cos\Lambda} - \frac{t/c}{\cos^2\Lambda} - \frac{C_L}{10\cos^3\Lambda} \tag{2}$$

M_{DD} is the drag divergence Mach number and was selected such that at cruise it would be a minimum. Λ is quarter chord sweep and K_a represents an airfoil technology factor. For supercritical airfoils, the technology factor is 0.95, and for NACA 6-series airfoils, the technology factor is 0.87. Geometric twist and taper ratio were coupled and used to try to obtain an elliptical lift distribution on the wing. Athena Vortex Lattice (AVL) was used to predict the relative efficiency between wings and converge on the best.

D. Drag

Four different methods were used to obtain a drag polar for this aircraft. The skin friction drag was modeled using flat plate approximations. The wave drag was modeled using a simple wave drag approximation equation. The induced drag was modeled using Athena Vortex Lattice[18] (AVL) code written by Mark Drela. And lastly the viscous drag due to lift was calculated using a 2D CFD study.

Flat plate skin friction approximations were used to analyze skin friction drag[19]. The flat plate friction coefficient was calculated using the fully turbulent mean skin friction coefficient. Next, the wing parasite drag was calculated using Equation 3.

$$C_{D,o,wing} = C_f\left[1 + 1.2\frac{t}{c} + \left(\frac{t}{c}\right)^4\right]\frac{S_{wet}}{S_{ref}} \tag{3}$$

Similarly, the horizontal and vertical tail surfaces zero-lift drag coefficients (C_{Do}) were calculated as well as the fuselage zero-lift drag coefficient.

The shock-induced drag for this aircraft was approximated using a simple wave drag equation. First, the critical Mach number (M_{crit}) was calculated using Equation 4 from the chosen M_{DD}.

$$M_{crit} = M_{DD} - \left(\frac{0.1}{80}\right)^{1/2} \tag{4}$$

Once the M_{crit} was known, the shock-induced drag was calculated using Equation 5 for Mach numbers greater than the M_{crit}.

$$C_{D,wave} = 20(M - M_{crit})^4 \frac{S_{strip}}{S_{ref}} \tag{5}$$

where S_{strip} is the reference area of a section of the wing, which lets the wave drag be summed over many strips rather one big block. This method was then compared to a CFD study where each Mach number between 0.65 and 0.91 at 0.02 intervals was evaluated. This resulted in the 2-D Mach drag divergence graph shown in Figure 6. The CFD was compared to the wave drag formula mentioned above. The graph shows that the wave drag equation under predicts the M_{DD} number. The CFD was then curve fitted and used as the wave drag for this aircraft because it gave more conservative results. This affected the cruise drag buildup in that there was very little shock-induced drag. Although M_{DD} was selected to minimize cruise drag, there is historically more shock-induced drag at the cruise point.

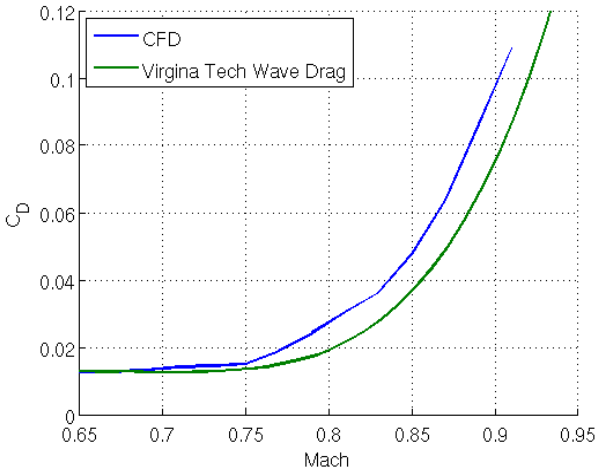

Figure 6: Mach Drag Divergence Graph Comparing CFD to Virginia Tech's Wave Drag Equation

The induced drag was calculated using AVL, which uses single layer vortex sheets that are curved along the camber line. Its limitations include that it works best at low angles of attack and sub-transonic Mach numbers. It uses the Prandtl-Glauert correction factor in the transonic regime, but a certain amount of unknown error is associated with Mach numbers above 0.7.

The viscous drag due to lift is calculated using 2D CFD analysis on the airfoil. Since the root and tip have different thickness to chord ratios, the two airfoils were interpolated to give a modified airfoil. The airfoil in the study used an 12% thickness to chord for NASA's SC-206 series airfoil. Since this is 2D analysis, the Reynolds number needs to reflect the local velocity that the 30 degree swept wing planform sees. The analysis was performed for cruise approximations at Mach number 0.68 at 38,000 feet and for takeoff at Mach number 0.20 at sea level conditions

The L/D_{max} for *Verde* is 18.1 which matches very closely to the L/D_{cruise} of 17.8. The two match closely because during the mission analysis the altitude for cruise was picked based on the least amount of fuel burned. This allows *Verde* to match its cruise altitude to its AR and cruise at its most efficient point altitude. The reason that these are not matching perfectly is because it was limited to cruise at 1,000 ft intervals. The cruise altitude for *Verde* on the 500 nmi mission is 38,000 feet.

E. Takeoff and Landing

To get the takeoff and landing performance of this aircraft an approximation of the aerodynamics of the flap system needs to be made. This maximum C_L was 2.75 for landing. This was low enough that a double slotted Flowler flaps would be able to achieve the necessary lift for the aircraft. The lift curves were made using a combination of a few methods and the resulting curves can be seen in Figure 7. First, 2D CFD was performed on the SC-20613 at a range of different angles of attack to get the 2D lift curve for

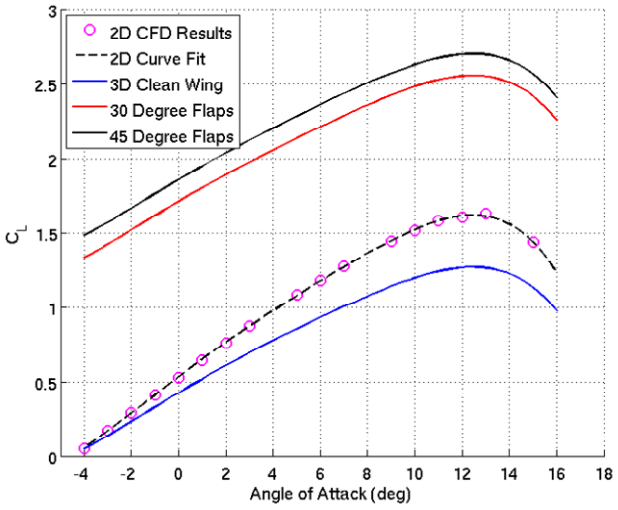

Figure 7: Lift Curve Slope for Different Flap Deflections.

that airfoil represented by the pink circles. A curve was fit to those results and then a 3D correction was made using a method from Raymer[20]. Lastly, a double slotted Fowler flap approximation was made using Roskam[15] for both 30 and 45 degree flap deflections. And from these the resulting drag polars for takeoff and landing can be determined.

F. Airfoil Study

To show a comparison of natural laminar flow airfoils to supercritical airfoils some values are listed in Table III. The airfoil study included all airfoils to be run under fully turbulent conditions which would be the worst case scenario for those airfoils. The Mach numbers are different because the natural laminar flow airfoils are run for a 20 degree swept wing where the local velocity of the airfoil would be 0.73. All drag predictions were run using CFD.

Table III: Airfoil Comparison for Supercritical and Natural Laminar Flow Airfoils.

Airfoil	$C_{L\ design}$	Mach Number	AoA (deg)	$C_{L\ cruise}$	$C_{d\ cruise}$	t/c
SC-20612	0.6	0.68	0.3	0.58	0.0099	12%
SC-20614	0.6	0.68	-0.11	0.60	0.0151	14%
HSNLF-213	0.2	0.73	3.6	0.62	0.0234	13%
NL(S)-0715	0.7	0.73	-0.4	0.60	0.0202	15%

As shown in Table III, the natural laminar flow airfoils perform quite poorly under fully turbulent conditions. Two supercritical airfoils are use, a t/c of 12% at the tip and 14% at the chord. Kermit Design wanted to analyze the airfoil so they performed basic 2D CFD analysis. Three cases were run for each Mach number at an altitude of 38,000 feet.

8. Performance

A cruise altitude study was completed to find the altitude where the lowest block fuel burn is achieved for a 500 nmi mission. From this, 38,000 ft was used as the cruise altitude, which gives a block fuel burn of 38.1 lb/seat for a 500 nmi mission.

9. Emissions

Due to the lower fuel burn, *Verde* accomplishes the carbon dioxide and nitrogen oxide emission reductions required by the RFP. But this does not fully satisfy the goals of Kermit Design, nor the future needs of the airline industry. As the demand for fuel increases worldwide with developing countries, the airline industry will soon be forced to consider introducing biofuel into a standard jet fuel mixture. This will assist not only the overall reliance of fossil fuels but also take another step forward in environmental responsibility.

10. Noise

The RFP proposes a significant reduction in the community noise of the aircraft. For an aircraft with a MTOW of 139,000 lb the cumulative noise requirement is 251 dB. The open rotor engine selection is louder than its competition turbofan engines, but still has the potential to employ many technologies. Noise reduction will look primarily to the engine, because it is the largest source of noise on the aircraft plays the most significant role in reducing overall noise.

For an open rotor engine, the propeller produces the most significant amount of noise from the engine. A propfan noise estimation from Hamilton Sundstrand[6] resulted in an engine noise level of 93 dB. General Electric predicts the next generation unducted fan to be about 10 dB below Stage 4. These improvements would come from advancements in blade design as well as the number coupling of the front and back rows of counter-rotating blades, odd number coupling and using different numbers of blades between the front and back rows help attenuate frequencies produced by the blades. Therefore, a 10 dB reduction was taken from the baseline noise estimation at each measurement location.

NASA's Aircraft Noise Prediction Program[21] (ANOPP) was used to quantify airframe noise. The unducted fan could not be modeled in ANOPP, therefore the *Verde* configuration was modeled along with a 737-800 for

comparison and validation. The ANOPP model appeared to under predict flyover noise and over predict approach, but cumulatively was within 0.5% of the actual noise levels of the 737-800.

Compared to the engines, airframe noise is less impacting to the overall noise level. On approach, the airframe noise reductions from clean double slotted flower flaps and clean landing gear do benefit the overall noise level. The logarithmic summation of the engine and airframe noise results in a cumulative noise level for *Verde* of 250.8 dB, which is 20.1dB below Stage 4.

11. Controls and Stability

The initial size of the horizontal tail was determined using a Roskam[22] volume coefficient method and was constrained by takeoff rotation, as shown in Figure 8. Using a tail volume coefficient of 1.25, the area of the horizontal tail was determined from Equation 7 to be 215 sq ft.

$$S_H = \frac{V_H \cdot \bar{c} \cdot S}{X_H} \tag{7}$$

However, after performing a dynamic stability analysis, it was found the damping ratio, ζ, for the short period mode was 0.23. This falls into a Level 2 handling quality[23], an unacceptable value for a commercial transport. In order to meet the minimum damping ratio requirement for Level 1 handling of 0.30, the horizontal tail size was increased to 295 sq ft. This yielded a tail volume coefficient of 1.71, which is higher than comparable aircraft in this class. This is most likely due to the high aspect ratio wing, which in turn creates a smaller mean aerodynamic chord, yielding a higher value of V_H for a comparably sized tail area.

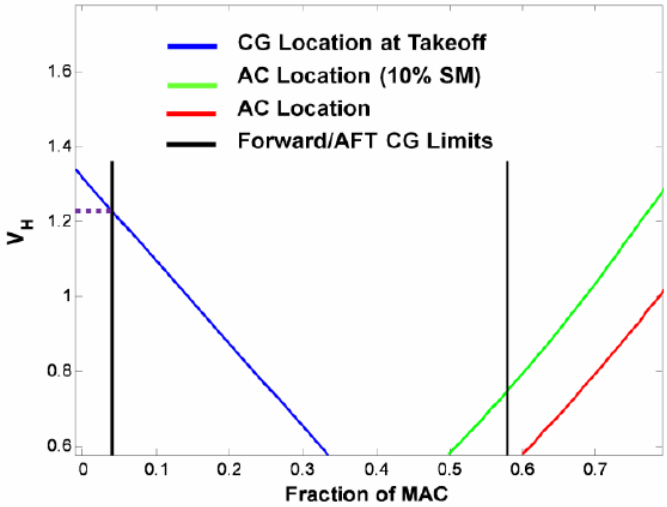

Figure 8: Horizontal tail sizing constraints.

The elevator was sized to provide the horizontal tail with a lift coefficient of -1.0 at takeoff. This was done using the plain flap method from Raymer[20], taking into account ground effect, downwash and 3D effects. The elevator chord was chosen to be 0.3 of the chord of the horizontal tail, which required an elevator deflection of about 13 degrees at takeoff. The horizontal tail span and taper were set to match the tip chord of the vertical tail, which yielded a span, taper ratio and aspect ratio of 40 ft, 0.38, and 5.4, respectively. The sweep of the horizontal tail was chosen to be just slightly higher than that of the wing, to prevent shock waves from forming on the control surfaces.

The size of the vertical tail was also determined by volume coefficients constrained the one-engine-inoperative (OEI) condition. Using an approximation for windmill drag from Torenbeek[13], the required directional stability coefficient (Cn,req) of 0.052 rad^{-1}, the rudder size and corresponding vertical tail size were chosen at a balanced point to attempt to minimize both the rudder size and vertical tail size. The vertical tail volume coefficient and rudder size were 0.073 and 0.25 $\bar{c}_v$.

As determined by Equation 8, the *Verde* required a vertical tail area 200 sq ft. The span of the vertical tail was chosen to be 15 ft., near that of the MD-80, as to allow adequate clearance of the engine fan blades, and allow for airport compatibility. The sweep of the vertical tail is 38°, as this provides enough sweep to prevent shocks from forming on the control surface.

$$S_V = \frac{V_V \cdot b \cdot S}{X_V} \tag{8}$$

The outboard ailerons span from 80% to 95% of the half-span, at 20% of the local chord, which yielded an aileron area of 54 ft^2 per aileron. Inboard ailerons to use during high speed maneuvers to prevent aileron reversal and extreme stress and torsion on the wing during flight have not been designed at this point, but Kermit Design will incorporate these.

Using Roskam[22], a trim triangle was created for the *Verde* at cruise condition. The *Verde* is stable and trimmable at all CG locations during cruise, requiring an elevator deflection between -5° and 7°. The stability derivatives for *Verde* were found using methods from Nelson[23] and Roskam[22], which were input into Archangel, where the dynamic stability characteristics were obtained. All of the dynamic response modes give a Level 1 handling quality.

12. Cost

The acquisition cost of *Verde* was determined using ALCCA[24]. Before the actual cost was determined, it was desired to study the effects of using advanced materials on *Verde*, and to see what factors would most heavily influence the total acquisition cost. An automation of ALCCA was created, to vary the percentage of titanium, aluminum, and composite materials used in the aircraft. Figure 9 shows a carpet plot of how the acquisition cost changes with increasing titanium and composite materials, relative to a decrease usage in aluminum material. From this plot, the sensitivity derivatives, or the slope of the contours in Table IV, were found for varying material usage in the fuselage and wing, as these two structural components constitute nearly 80% of the aircraft structural cost. From this sensitivity study, it was concluded that the acquisition cost of the aircraft was much more sensitive to an increase in usage of composite materials. However, as will be discussed later, the long-term operating benefits of composites will more than buy their way onto *Verde*'s design.

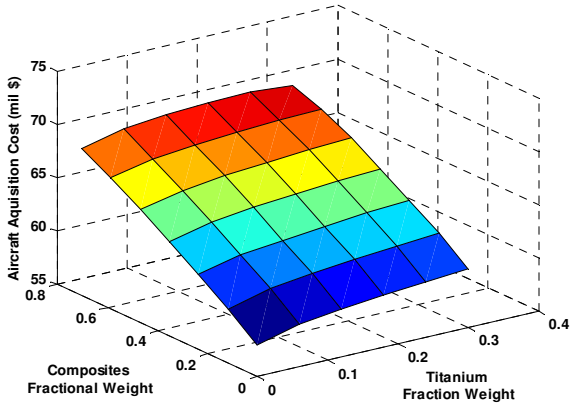

Figure 9: Acquisition Cost Variation with Material Usage

Table IV: Acquisition Cost Sensitivity to Advanced Material Usage

Parameter	Sensitivity
$\frac{\partial \$Aq}{\partial \%Ti_{wing}}$	0.023 mil.
$\frac{\partial \$Aq}{\partial \%Comp_{wing}}$	0.103 mil.
$\frac{\partial \$Aq}{\partial \%Ti_{fuselage}}$	0.080 mil.
$\frac{\partial \$Aq}{\partial \%Comp_{fuselage}}$	0.150 mil.

As a baseline for predicting the acquisition cost, values of 50% composites, 20% titanium and 30% aluminum on the fuselage, and 40% composites, 30% titanium, and 30% aluminum on the wing were used. This yielded an acquisition cost of approximately $88.5 million for 500 units produced, and $63.6 million for 1,500 units produced. This is well below the actual cost of a Boeing 737-800, but just slightly below the Boeing 737-800 estimated cost, which was also estimated using ALCCA.

While the airline industry faces such unpredictable economic times, decreasing the operating cost is of the utmost importance. It was also Kermit Design's philosophy that the most feasible way to drastically reduce operating from a conceptual design view, was to dramatically reduce fuel burn. This was accomplished through selection of the unducted fan engine cycle and the used of advanced materials to reduce the weight of *Verde*. Using ALCCA to predict the operating cost of *Verde*, the total direct operating cost averaged to $2,100 per block hour (in 2018 dollars). In order to determine how much of an impact fuel cost had on operating cost, several parameters were found for three different years, including the present year (2009), and the RFP entry to service date of 2018. These parameters included inflation, fuel prices, and direct operating cost. Table V shows a summary and comparison of these parameters. From the year 2000 to 2018, inflation is projected in increase by about 54%, while fuel prices are predicted to increase by at least 257%. Assuming that maintenance costs and other operating cost (less fuel), are only affected directly by inflation, the fuel cost will vastly outpace inflation, implying that fuel will become a more and more dominate factor in direct operating cost. It is projected that *Verde* will reduce operating cost by 8.4% in 2009, but by the entry service date, will increase that to a 10.6% cost savings over a Boeing 737-800. This savings nets an average of nearly $1.7 million per year per aircraft, assuming 5,000 block hours per year. A benefit is also seen, although not as great, with *Verde*'s Leap 56 option. This option will result in approximately 4.7% savings in

operating cost over the 737-800 in 2018. While this is a far cry the RFP objective of 8%, it is still shows an improvement over current aircraft. The next generation aircraft has no other choice, but to go with the unducted fan cycle in order to keep up with rising fuel prices, and give airlines a chance to make a profit in an uncertain economic future.

Table V. Operating Cost Analysis

Parameter	2000	2009	2018
Inflation	---	24%	~54%
Fuel Prices[18] ($/gal)	0.70	1.39	2.50
Relative Fuel Price Increase	---	99%	257%
DOC Savings over B737-800	6.1%	8.4%	10.6%
DOC Savings over B737-800 (CFM option)	2.7%	3.8%	4.7%

13. Conclusion

Designed primarily to reduce fuel burn and emissions, *Verde* utilizes the balance of several green technologies such as an unducted fan engine cycle, biofuel, and use of advanced yet reusable materials. The fuel-burn-centered philosophy yielded significant improvements, including a fuel block burn for the typical 500 nmi mission of 38.1 lb/seat and an 10% improvement in operating cost compared to current standards. The use of advanced materials allows an increase in aspect ratio balanced with structural weight, aerodynamic performance benefits, and airport integration. All design decisions for *Verde* focused first on reducing fuel burn, second on reducing emissions, then noise, and finally on maintaining flyaway cost, airport integration, and passenger comfort. Further detail of this design process and the analysis can be found in an extended report online at: http://www.flightlab.calpoly.edu/html/design_reports/. Kermit Design is confident *Verde* is the solution to successfully carry the 150-passenger commercial class of aircraft through the industry demands for reduced fuel burn and environmental responsibility.

Acknowledgments

The authors would like to thank the individuals from Boeing, Lockheed Martin, Northrop Grumman, Edwards Air Force Base, and the 2009 Cal Poly Aerospace Symposium guests for their reviews and feedback throughout this conceptual design.

References

[1] American Institute of Aeronautics and Astronautics. Request for Proposal, "Advanced, Environmentally Compatible, 150-seat Commercial Transport." Undergraduate Team Aircraft Design Competition. 2008-2009.

[2] Environmentally Responsible Aviation Project About Us, NASA, Integrated Systems Research Program, <http://www.aeronautics.nasa.gov/isrp/era/index.htm >.

[3] Bradley, Kevin R. "A Sizing Methodology for the Conceptual Design of Blended-Wing-Body Transports." NASA CR- 2004-213016, George Washington University Joint Institute for the Advancement of Flight Sciences Langley Research Center, Hampton, Virginia, Sept. 2004.

[4] Ciszek, Raymond Scott. "Prop Fan Propulsion Concepts: Technology Review, Design Methodology, State-of-the-Art Designs and Future Outlook." University of Virgina Department of Mechanical and Aerospace Engineering. Senior Thesis Project. March 25, 2002.

[5] GE Aircraft Engines, GE36 Project Department. "Full Scale Technology Demonstration of a Modern Counterrotationg Unducted Fan Engine Concept." NASA. Cincinnati, Ohio, December 1987.

[6] "Large Scale Advanced PropFan (LAP) Performance, Acoustic and Weight Estimation." NASA Contractor Report CR-174782, February 1985.

[7] Baum, J.A., Dumais, P.J., Mayo, M., Metzger, F.B., Shenkman, A.M., Walker, G.G. "Prop-fan Data Support Study," NASA-CR-152141, February 28, 1978.

[8] Wainusky, H.S. and Vaczy, C.M., "Aerodynamic Performance of a Counter Rotating Prop-Fan," AIAA Paper 86-1550, 1985.

[9] Mecham, Michael and Wall, Robert. "Beyond LEAP."*Aviation Week & Space Technology.* May 25, 2009.

[10] Roskam, J., *Airplane Design Part II-V, DAR Corporation*, Lawrence, KS, 1989.
[11] York, P., Labell, R., "Aircraft Wing Weight Build-Up Methodology with Modification for Materials and Construction Techniques CR 166173", National Aeronautics and Space Administration, Moffett Field, CA, 1980.
[12] *Introduction to Aircraft Weight Engineering*, Society of Allied Weight Engineers. SAWE INC., Los Angeles, CA, 1996.
[13] Torenbeek, E., Synthesis of Subsonic Airplane Design, Delft Univ. Press, Delft, The Netherlands, 1982.
[14] "DC-10 40 Flight and Engineering Manual", McDonnell Douglas Corporation.
[15] Roskam, Jan, and C. T. Lan. *Airplane Aerodynamics and Performance.* Lawrence: DARcorporation, 2000.
[16] Flight Optimization System (FLOPS) Release 7.41, NASA Langley Research Center, Hampton, VA 23681-0001, 18 December 2008.
[17] W.H. Mason, "Analytic Models for Technology Integration in Aircraft Design," AIAA Paper 90-3262, September 1990.
[18] Athena Vortex Lattice Code (AVL) 3.26 User Primer. Mark Drela. MIT Aero and Astro. 29 Apr 2006.
[19] Aircraft Aerodynamics and Design Group Stanford, "Aircraft Structural Design." 17 Mar 2009 <http://adg.stanford.edu/aa241/structures/structuraldesign.html>.
[20] Raymer, D. P., *Aircraft Design: A Conceptual Approach*, American Institute of Aeronautics and Astronautics, Inc., Reston, VA, 2006.
[21] Gillian, Ronnie E. "Aircraft Noise Prediction Program User's Manual," NASA Technical Memorandum 84486, Langley Research Center, Hampton, Virgina 1982.
[22] Roskam, J., *Airplane Flight Dynamics and Automatic Flight Controls*, DAR Corporation, Lawrence, KS, 2007.
[23] Nelson, R. C., *Flight Stability and Automatic Control*, McGraw-Hill Companies Inc., Boston, MA, 1998.
[24] Aircraft Life Cycle Cost Analysis (ALCCA) Military and Commercial Version 7, Aerospace Systems Design Laboratory, Georgia Tech, Atlanta, GA. Feb 2004.